Tritium and helium release from beryllium pebbles neutron-irradiated up to 230 appm tritium and 3000 appm helium

Vladimir Chakin*, Rolf Rolli, Pavel Vladimirov, Anton Moeslang

Karlsruhe Institute of Technology, Institute for Applied Materials, Hermann-von-Helmholtz-Platz 1, 76344 Eggenstein-Leopoldshafen, Germany

A B S T R A C T

Study of tritium and helium release from beryllium pebbles with diameters of 0.5 and 1 mm after high-dose neutron irradiation at temperatures of 686–968 K was performed. The release rate always has a single peak, and the peak temperatures at heating rates of 0.017 K/s and 0.117 K/s lie in the range of 1100–1350 K for both tritium and helium release. The total tritium release from 1 mm pebbles decreases considerably by increasing the irradiation temperature. The total tritium release from 0.5 mm pebbles is less than that from 1 mm pebbles and remains constant regardless of the irradiation temperature. At high irradiation temperatures, open channels are formed which contribute to the enhanced tritium release.

© 2016 The Authors. Published by Elsevier Ltd.
This is an open access article under the CC BY license (http://creativecommons.org/licenses/by/4.0/).

1. Introduction

Beryllium is considered to be used as a neutron multiplier material in a form of pebbles with a diameter of 1 mm in the helium cooled pebble bed (HCPB) breeding blanket of ITER and DEMO [1,2]. In the fusion reactors, the beryllium pebbles will be irradiated by high fluxes of fusion neutrons resulting in the production of significant amounts of tritium and helium atoms. The beta-radioactive tritium accumulated in the pebbles to the end-of-life (EOL) of the blanket complicates handling of the beryllium waste. Most likely, helium plays a key role in mechanisms of radiation damage of beryllium under neutron irradiation, in particular, in the tritium retention. Therefore, tritium and helium release tests of beryllium pebbles irradiated in the HFR, Petten, the Netherlands, were chosen as a mandatory step of post-irradiation examinations (PIE).

The objective of this study is to establish regularities of tritium and helium release behavior in neutron-irradiated beryllium in connection with radiation-induced changes in the microstructure.

2. Experimental

Beryllium pebbles with diameters of 0.5 and 1 mm used at this study have been produced in NGK Insulators, Japan, by rotating electrode method (REM). The pebbles were irradiated within the HIDOBE-01 experiment in the High Flux Reactor (HFR) at temperatures of 686, 753, 861, and 968 K up to 1890, 2300, 2680, 2950 appm helium and 142, 172, 203, 230 appm tritium accumulation, correspondingly [3–5]. The tritium and helium accumulation calculations have been performed using the FISPACT code [6] for the adjusted neutron spectrum at the position of each activation monitor set in the HIDOBE-01 capsule.

Temperature-programmed desorption (TPD) tests were performed using a flow-through setup with a quadrupole mass-spectrometer (QMS) and an ionization chamber (IC). The setup is located in a glove box filled with high purity nitrogen. The mixture of high purity argon with a small addition of hydrogen $(Ar + 0.1 \text{ vol.\% } H_2)$ was used as a purge gas to transport the species released from the furnace to the QMS and the IC. The addition of small amount of hydrogen to the purge gas in the flow-through setup significantly facilitates the tritium desorption due to formation of the $^1H^3H$ molecule which easier escapes the beryllium surface compared to the $^3H_2$. The flow rate of the purge gas was 10 ml/min. The gas flow with released species moves to a Zn-bed heated to 663 K which transforms tritium water to tritium gas to avoid tritium water absorption in the pipes and in the IC. For the same reason, the gas pipes in the manifold are heated to 573 K during the TPD tests. Weight of the pebbles per each TPD test was in a range from 0.008 to 0.015 g that corresponded to 8–12 pebbles with 1 mm diameter or 90–120 pebbles with 0.5 mm diameter packed in the test cell. Each set of the beryllium pebbles (differing in diameter and irradiation parameters) was divided into two subsets, which were heated during the TPD test with 0.017 and 0.117 K/s, respectively. In all cases, the heating ramp started from the room temperature and run up to 1373 K with exposure at the maximum temperature for 3 hours. A detailed description of

* Corresponding author.
  E-mail address: vladimir.chakin@kit.edu (V. Chakin).

the flow-through setup and the technique used in the TPD tests is given in [3].

Preparation of irradiated beryllium pebbles for optical microscopy study has been performed by placing them in a resin layer on a sample holder. Then, the pebbles in the holder were grinded and polished until half of the pebble remains. The prepared cross sections of the pebbles were investigated using optical microscope (OM) Olympus GX51 placed in a glove box.

3. Results

3.1. Tritium and helium release

The release rate of tritium as well as helium for all tested irradiated beryllium pebbles has a single peak which is located at temperatures lower than the maximum testing temperature of 1373 K. Fig. 1a and b show examples of measured thermal desorption curves at heating rates of 0.017 K/s and 0.117 K/s, accordingly, for both tritium and helium released from the pebbles with a diameter of 0.5 mm irradiated at 753 K. Fig. 1c and d show results of the same thermal desorption tests presented separately for tritium and helium release, accordingly, as a function of temperature. The peak for the pebbles tested at 0.117 K/s is located at higher temperatures than that for pebbles tested at 0.017 K/s. Two corresponding helium release peaks have the similar relative location. This observation, that a higher heating rate causes a higher peak temperature for both tritium and helium, is common for almost all TPD test performed in this study. We will characterize the result of each TPD test by the peak temperature and the total release (the peak area). This allows comparing the TPD test results with each other.

There are some features in the shape and the mutual location of the peaks for beryllium pebbles irradiated at the highest temperature of 968 K (Figs. 2 and 3). In particular, for 0.5 mm pebbles, the tritium and helium release peaks have a narrow shape (Fig. 2a and b), and these peaks show lower tritium release rates (Fig. 2c and d) compared to lower irradiation temperatures). Besides that, both helium release peaks (after 0.017 and 0.117 K/s) practically coincide with each other (Fig. 2d), i.e. they have almost the same peak temperature. Concerning the 1 mm pebbles irradiated at 968 K, the tritium release peaks have also a narrow shape (Fig. 3a and b), and significantly lower heights compared to lower irradiation temperatures (Fig. 3c). Compared to the tritium peaks, the helium release peaks have a normal rounded shape (Fig. 3d).

Fig. 4 shows the plot of the tritium release peak temperature versus the irradiation temperature for all the TPD tests performed. For each set of pebbles in terms of pebble size and heating rate, the tritium release peak temperature is almost constant up to the irradiation temperature of 861 K. In contrast, at the highest irradiation temperature of 968 K, the tritium release peak temperature demonstrates an irregular behavior (an increase for 1 mm pebbles and a decrease for 0.5 mm pebbles). Correspondingly, the helium release peak temperature (Fig. 5) decreases slightly with increasing the irradiation temperature for all tests up to the temperature of 861 K, while at the highest irradiation temperature of 968 K the helium release peak temperature shows a similar irregular behavior as that of tritium.

Fig. 6 shows the total tritium release from the beryllium pebbles versus irradiation temperature. There is a difference in the total release from 0.5 mm and 1 mm pebbles with respect to the irradiation temperature. The total tritium release from 0.5 mm pebbles is lower than that from the 1 mm pebbles and has a constant (or slightly decreasing) value for each heating rate with increasing irradiation temperature. The total tritium release from the 1 mm pebbles significantly decreases with the increasing irradiation temperature. The difference in the total release from the 1 mm pebbles
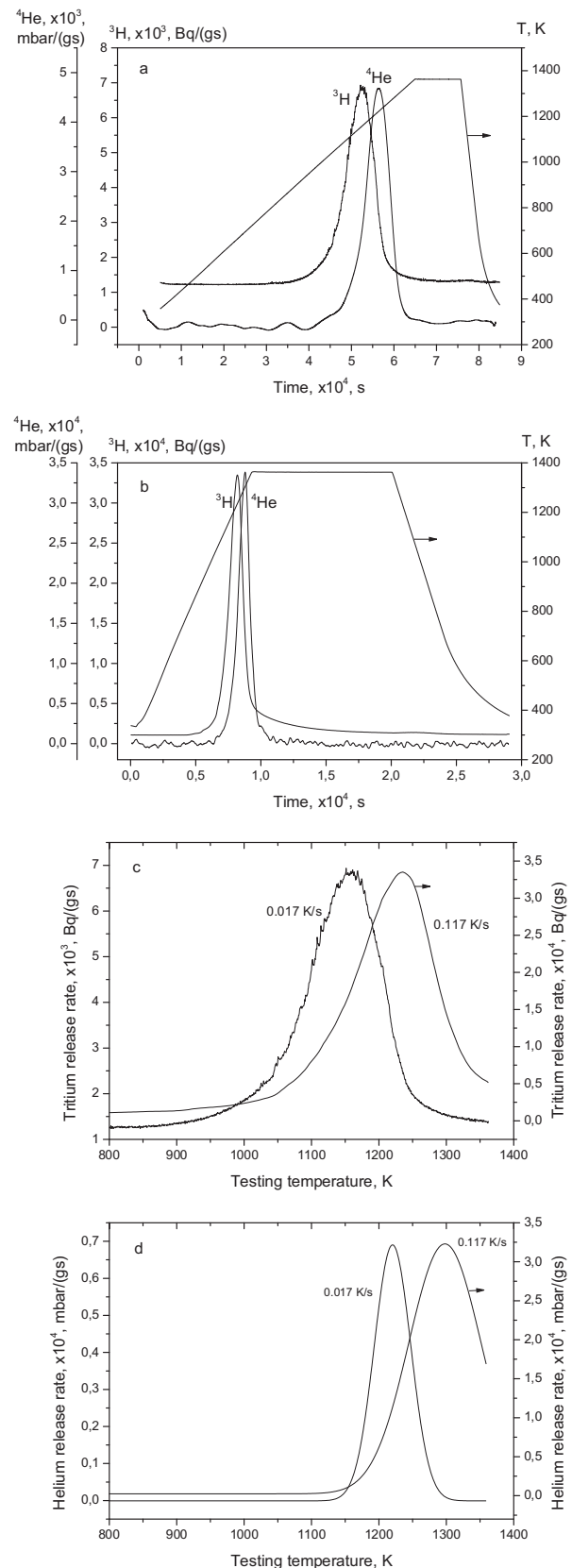

Fig. 1. Tritium and helium release rate for 0.5 mm beryllium pebbles after irradiation at $T_{irr} = 753$ K: (a) tritium ^{3}H and helium ^{4}He release rate at heating rate of 0.017 K/s versus time and temperature; (b) tritium ^{3}H and helium ^{4}He release rate at heating rate of 0.117 K/s versus time and temperature; (c) tritium ^{3}H release rate at heating rates of 0.017 K/s and 0.117 K/s versus temperature; (d) helium ^{4}He release rate at heating rates of 0.017 K/s and 0.117 K/s versus temperature.
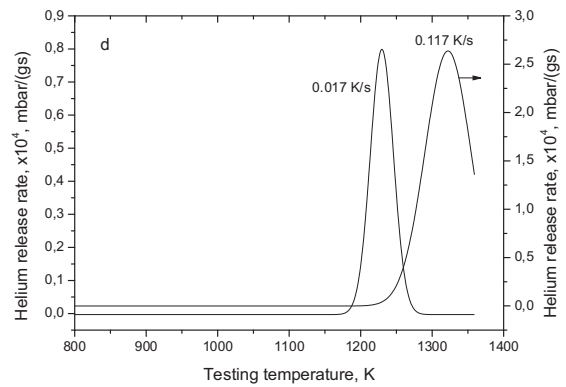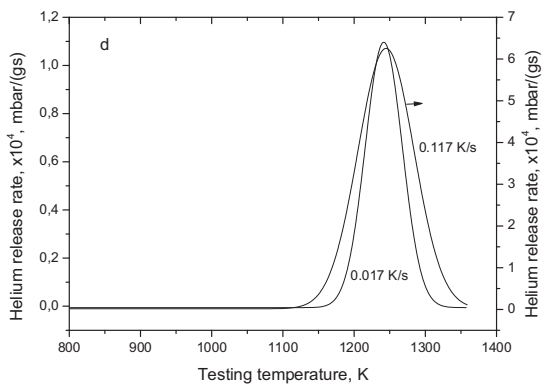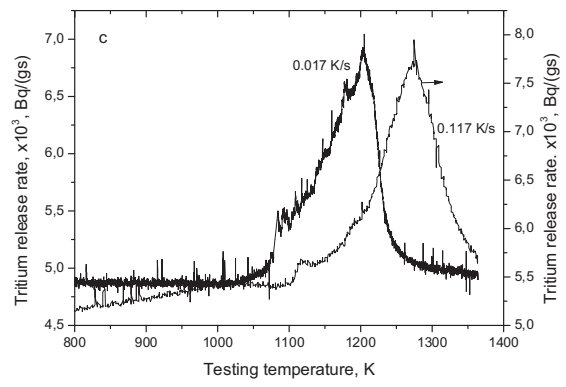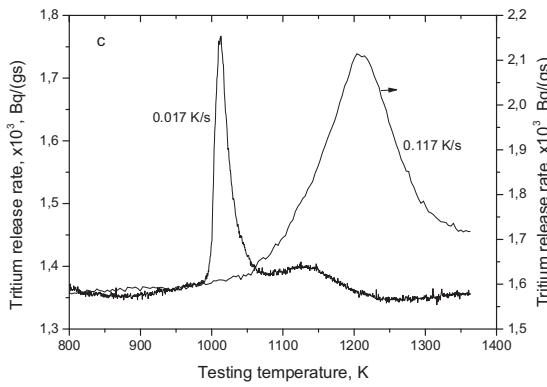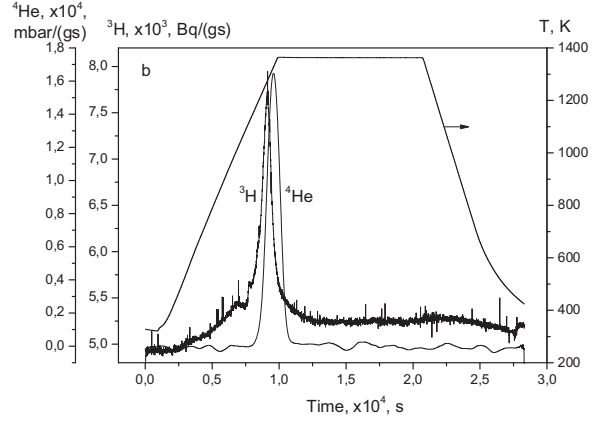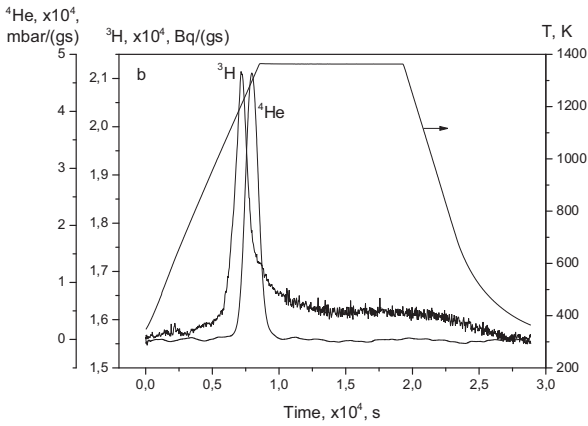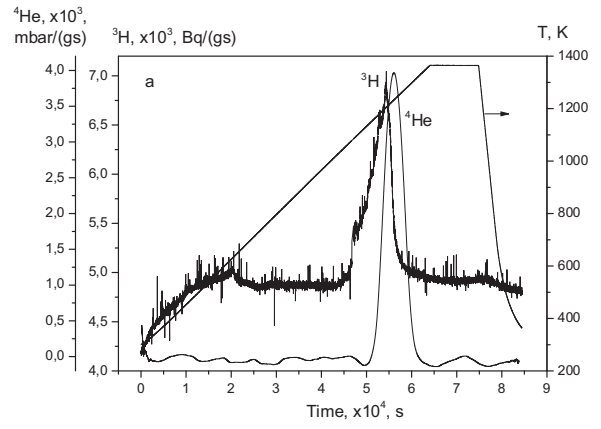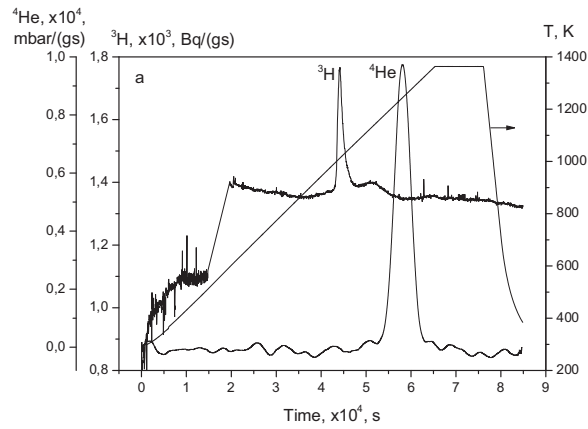
Fig. 2. Tritium and helium release rate for 0.5 mm beryllium pebbles after irradiation at $T_{irr} = 968$ K: (a) tritium ^{3}H and helium ^{4}He release rate at heating rate of 0.017 K/s versus time and temperature; (b) tritium ^{3}H and helium ^{4}He release rate at heating rate of 0.117 K/s versus time and temperature; (c) tritium ^{3}H release rate at heating rates of 0.017 K/s and 0.117 K/s versus temperature; (d) helium ^{4}He release rate at heating rates of 0.017 K/s and 0.117 K/s versus temperature.

Fig. 3. Tritium and helium release rate for 1 mm pebbles after irradiation at $T_{irr} = 968$ K: (a) tritium ^{3}H and helium ^{4}He release rate at heating rate of 0.017 K/s versus time and temperature; (b) tritium ^{3}H and helium ^{4}He release rate at heating rate of 0.117 K/s versus time and temperature; (c) tritium ^{3}H release rate at heating rates of 0.017 K/s and 0.117 K/s versus temperature; (d) helium ^{4}He release rate at heating rates of 0.017 K/s and 0.117 K/s versus temperature.
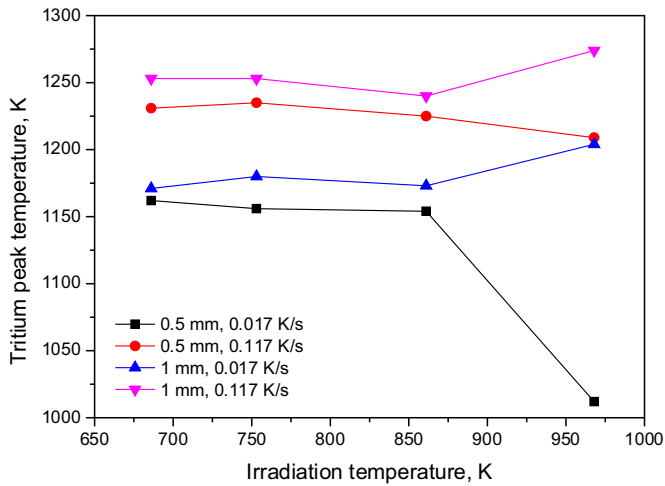
Fig. 4. Tritium peak temperature versus irradiation temperature for beryllium pebbles.
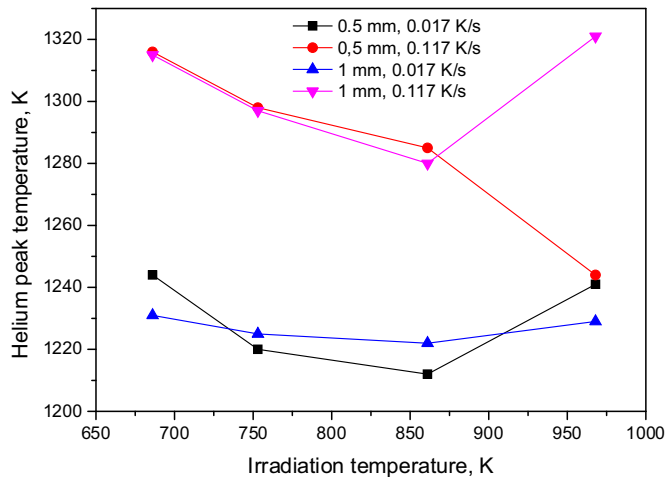

Fig. 5. Helium peak temperature versus irradiation temperature for beryllium pebbles.
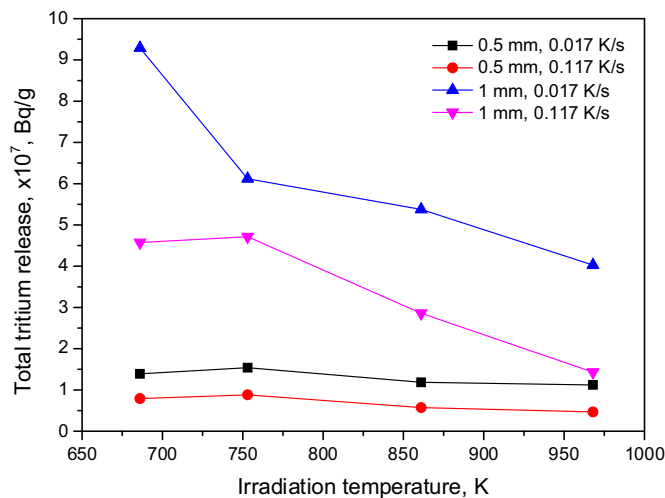

**Fig. 6.** Total tritium release from beryllium pebbles versus irradiation temperature.
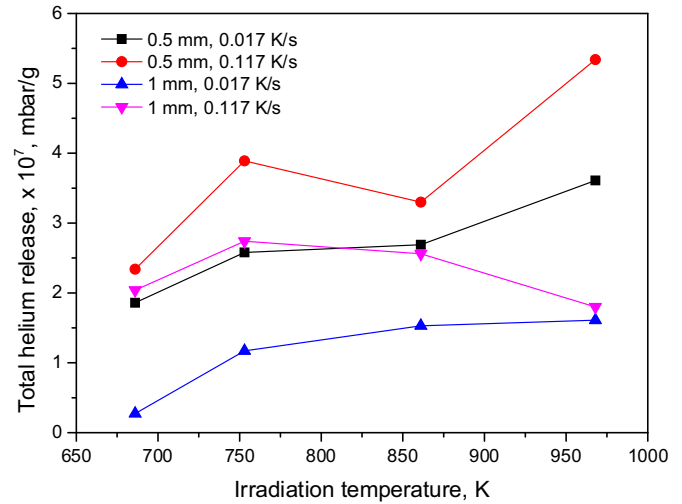
**Fig. 7.** Total helium release from beryllium pebbles versus irradiation temperature.
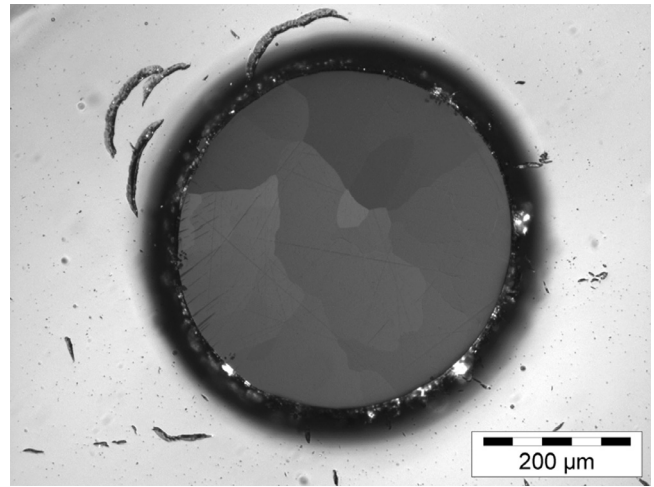
Fig. 8. Optical micrograph in polarized light of cross section of 0.5 mm beryllium pebble after irradiation at $T_{irr} = 686$ K.

tested at the 0.017 and 0.117 K/s heating rates is much more pronounced than from the 0.5 mm pebbles. For both pebble diameters, the total tritium release from the pebbles tested at the lower heating rate is comparatively higher than that at the higher heating rate.

Fig. 7 shows the total helium release from the pebbles versus the irradiation temperature. The main tendency here is the increase of the total helium release with increasing temperature (excluding the 1 mm pebbles tested at 0.117 K/s). This increase means a permanent helium accumulation in beryllium with increasing neutron fluence because according to the capsule design [4,5], the higher irradiation temperature of the pebbles in the capsule corresponds to the higher neutron fluence. From this point it can be concluded that helium produced under irradiation in beryllium remains in the pebble what completely differs from tritium, which can leave the pebble during irradiation at increasing irradiation temperatures.

3.2. Microstructure

Microstructures of the 0.5 mm beryllium pebbles irradiated at 686 K (Fig. 8) and at 753 K (Fig. 9) are similar to each other. For both irradiation temperatures, coarse grains with sizes up to 250 μm and absence of pores are the main features. At higher ir-
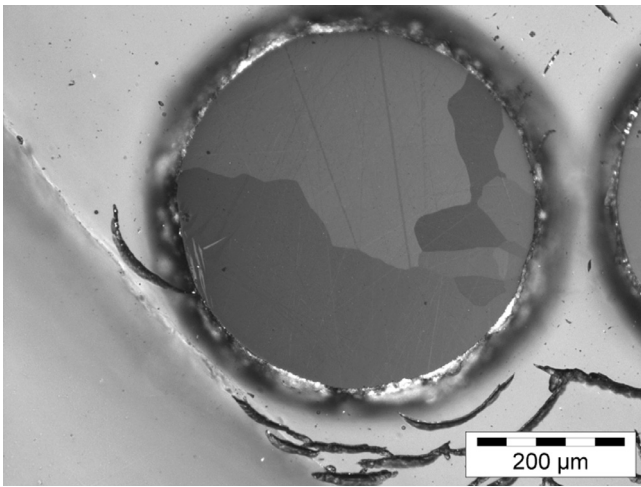
Fig. 9. Optical micrograph in polarized light of cross section of 0.5 mm beryllium pebble after irradiation at $T_{irr} = 753$ K.

radiation temperature of 861 K (Fig. 10a), the microstructure also consists of coarse grains but pores with sizes up to 25 μm are already observed. The pores have a faceted shape and are located mainly on grain boundaries (Fig. 10b). At the highest irradiation temperature of 968 K, numerous pores are present in the microstructure. Some of them have large sizes reaching 60 μm (Fig. 11a). Other pores have much smaller sizes of about 5 μm (Fig. 11b). The smaller pores have a rounded shape and can be identified as gas bubbles. The bubbles often are arranged in lines along grain boundaries which have denuded zones (up to 20 μm in width). Another feature of this microstructure is the presence of numerous ultra-fine bubbles located in vicinity of large pores.

The microstructure of 1 mm beryllium pebbles after irradiation at 686 K (Fig. 12a) is similar to the 0.5 mm pebbles irradiated at the same temperature (Fig. 8). In addition, small pores and cracks are sometimes present in the microstructure (Fig. 12b).

The 1 mm beryllium pebbles irradiated at higher temperature of 753 K (Fig. 13a) have a typical coarse grain structure. Separate small pores are visible in the grains close to the external pebble surface. Partial fragmentation of the coarse grains in smaller sub-grains occurs in the near-surface layers (Fig. 13b).

The microstructure of 1 mm beryllium pebbles after irradiation at 861 K (Fig. 14a) demonstrates presence of numerous large pores distributed quite evenly over the pebble cross section. A significant portion of the pores is located on the grain boundaries. The external surfaces of pebbles are covered with oxide layers having thickness up to 15 μm (Fig. 14b). Likely, this surface layer consists of beryllium oxide (BeO) phase. The BeO layer has a not dense and even loose structure.

After irradiation at the highest temperature of 968 K, the microstructure of 1 mm beryllium pebbles contains significant amount of large pores (Fig. 15). Some pebbles have pores in the internal regions as well as in the near-surface layers (Fig. 15a). In other pebbles, the pores are mainly collected in a region only which is close to the surface (Fig. 15b). Some pebbles contain the pores mainly in internal regions (Fig. 15c). Despite the differences in the pore location and distribution, open channels surrounded by denuded zones always are present in the microstructures as well as surface oxide layers (up to 20 μm thickness) (Fig. 15d).

4. Discussion

By using the approach suggested in [7] and developed in the application to different materials in [8–10], the rate of desorption
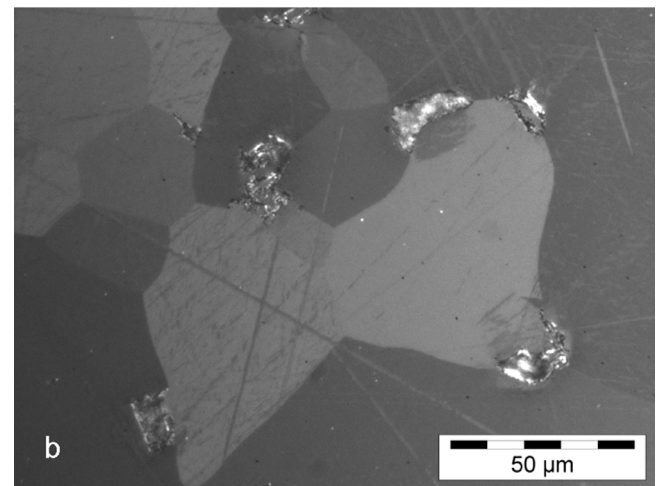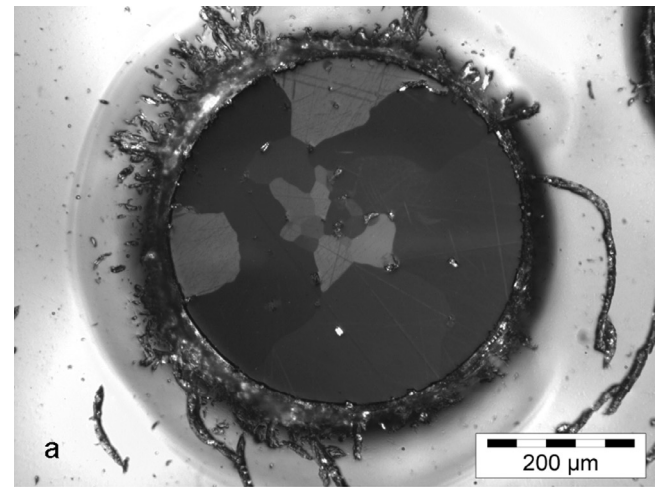

Fig. 10. Optical micrograph in polarized light of cross section of 0.5 mm beryllium pebble after irradiation at $T_{irr} = 861$ K: (a) coarse grains; (b) pores with faceted shape.

N (t) may be written as

$$N(t) = -d\sigma/dt = \nu_n \cdot \sigma^n \cdot \exp(-E_{des}/kT), \tag{1}$$

where n is the order of the desorption reaction; σ is the surface coverage; νn is the rate constant, s^{-1}; E_{des} is the desorption activation energy, eV.

We consider the linear change of a sample temperature T with time t such as

$$T = T_0 + \beta t, \tag{2}$$

where T_0 is the initial temperature, K; β is the heating rate, K/s. We also assume that Edes is independent of σ. The Eq. (1) can be solved to find the temperature (T_m) at which the desorption rate is a maximum. Then, for n = 1 (the first order reaction was chosen for the tritium desorption), we obtain

$$E_{des}/kT_m^2 = (\nu/\beta) \cdot \exp(-E_{des}/kT_m), \tag{3}$$

Making the logarithm from (3), we obtain

$$\ln(\beta/T_m^2) = \ln(\nu/\beta) \cdot -E_{des}/kT_m, \tag{4}$$

The desorption activation energy E_{des} can be determined by varying β and plotting $\ln(\beta/T_m^2)$ against $1/T_m$. This method was applied to calculate E_{des} for tritium release from the irradiated beryllium pebbles.

Fig. 16 shows the activation energy of tritium desorption from irradiated beryllium pebbles versus irradiation temperature. Averaging E_{des} separately for 0.5 mm pebbles and 1 mm pebbles, we
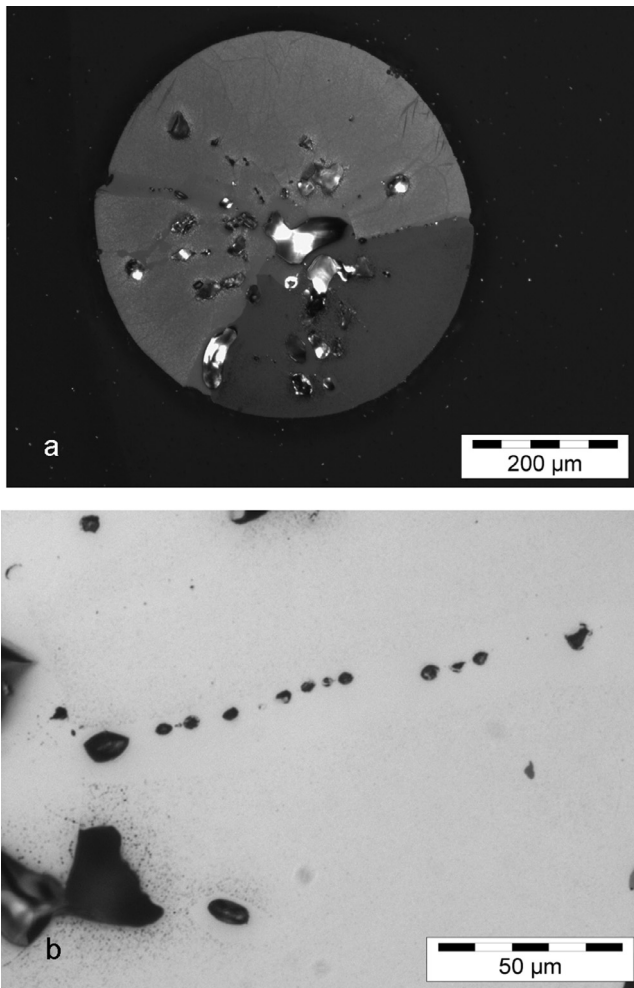
Fig. 11. Optical micrograph in polarized light of cross section of 0.5 mm beryllium pebble after irradiation at $T_{irr} = 968$ K: (a) large pores; (b) small bubbles arranged in lines along grain boundaries which are surrounded by denuded zone.
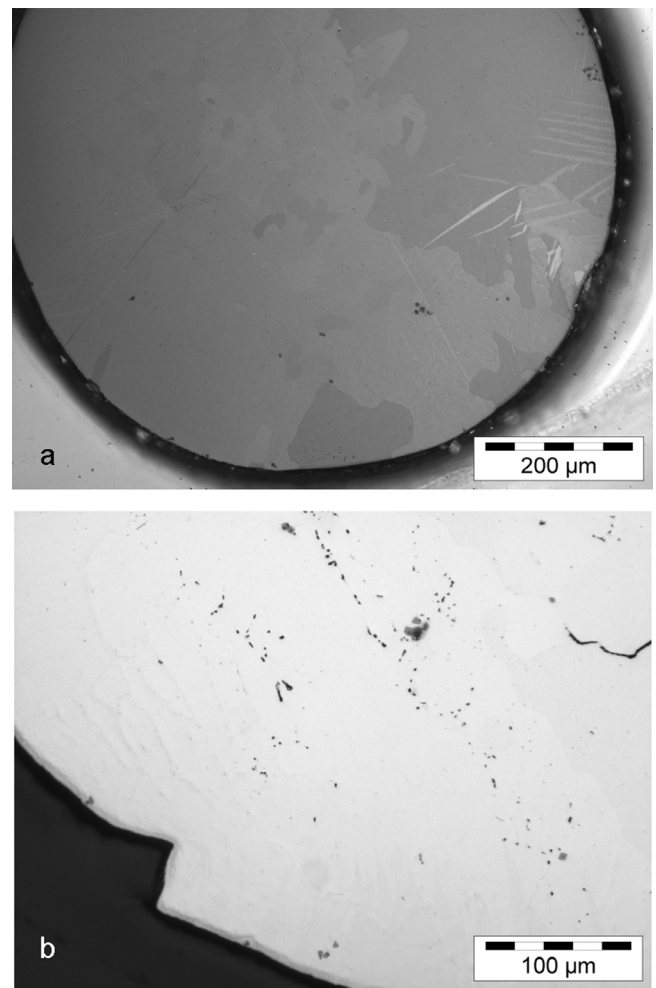
Fig. 12. Optical micrograph in polarized light of cross section of 1 mm beryllium pebble after irradiation at $T_{irr} = 686$ K: (a) coarse grains; (b) small pores and cracks.

obtain 2.5 eV and 2.9 eV, accordingly, regardless of the irradiation temperature. Taking into account a scattering in determining of the peak temperatures, the insufficient statistics in the TPD tests performance, and supposing that the structural traps for tritium are the same for both 0.5 mm and 1 mm pebbles, we estimate the average value of the activation energy of tritium desorption from the irradiated beryllium pebbles as $E_{des} = 2.7$ eV. It should be taken into account that the obtained E_{des} does not equal to an energy of tritium desorption from the beryllium surface E_D. E_{des} indicates (or overestimates if to take into account an input of tritium diffusion) the energy of tritium detrapping from the structural traps in the irradiated beryllium pebbles.

The microstructure of the beryllium pebbles irradiated at $T_{irr} = 686$–968 K contains numerous small gas bubbles with a hexagonal honeycomb shape [11]. These small bubbles are filled by helium and tritium gases produced in the beryllium pebbles under neutron irradiation. Large pores which are in the beryllium pebbles after production by the REM are filled by the transmuted tritium and helium. The obtained TEM results support the assumption about the same type of the structural traps in irradiated beryllium regardless of the pebble diameter.

The main chemical form of tritium in the neutron irradiated beryllium is a molecule $^3H_2$ [12] (see Fig. 17). This means that tritium in the molecular form fills both the radiation-induced small gas bubbles and the large pores. To leave a bubble or a pore, a

tritium molecule $^3H_2$, first of all, has to dissociate since tritium in the molecular form is not able to move through the beryllium bulk. The activation energy per atom for dissociation of a hydrogen molecule is 2.25 eV [13] however, the dissociation of $^1H_2$ (or $^3H_2$ if ignoring the isotope effect) on the beryllium surface can occur with the lower activation energy $E_{diss} = 0.8$ eV [14]. After dissociation, to leave the bubble and to penetrate to the bulk, the hydrogen (tritium) atom has to overcome a barrier E_A around 2.3 eV. This value has to exceed the energy of solution of hydrogen in beryllium E_S which is around 1 eV. The tritium migration in beryllium is very fast ($E_m = 0.2$–0.4 eV). Finally, to leave the pebble, tritium has to overcome a barrier $E_D = 0.8$ eV (the same as the activation energy for dissociation of a hydrogen molecule but this is the reverse situation to adsorption). Tritium on the pebble surface interacts with hydrogen from the purge gas (see Section 2) and leaves the surface in the form of the molecule $^1H^3H$.

The value of E_A taken from the potential diagram (2.3 eV) is close to that which was obtained using the TPD tests (2.7 eV). It should be once again emphasized that in our consideration, the isotope effect is ignored.

The tritium peak temperatures T_m for both 0.5 and 1 mm pebbles and for $T_{irr} = 686$–861 K are within 1150–1180 K for 0.017 K/s and 1230–1250 K for 0.117 K/s, i.e. very close to each other for every heating rate (see Fig. 4). At the maximum irradiation temperature of 968 K, T_m varies rather irregularly. Around the highest irradiation temperature of 968 K, which corresponds to $0.63T_{melt}$ (T_{melt}
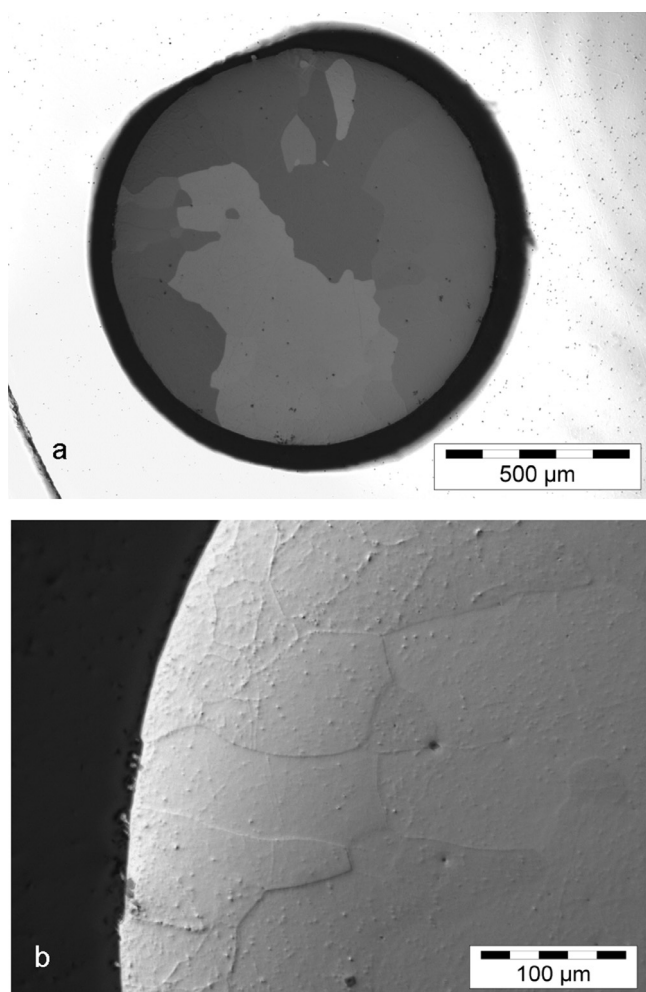
Fig. 13. Optical micrograph in polarized light of cross section of 1 mm beryllium pebble after irradiation at $T_{irr} = 753$ K: (a) coarse grains; (b) fragmentation of large grains to smaller sub-grains.
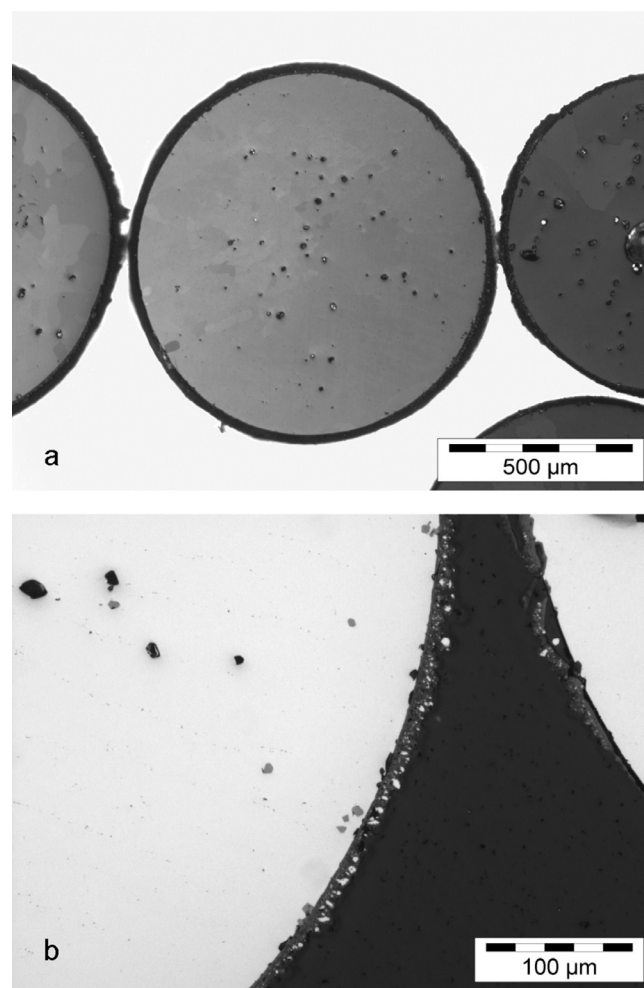
Fig. 14. Optical micrograph in polarized light of cross section of 1 mm beryllium pebble after irradiation at $T_{irr} = 861$ K: (a) pores in internal regions; (b) oxide layer on the pebble surface.

is the melting point of beryllium), the bubble density is so high that they form an open porosity network, i.e. open channels to the pebble surface are formed, through which tritium can easily escape the pebble [15–20] (see Fig. 15). Probably, the comparable peak temperatures for $T_{irr} = 686$–861 K are due to the same type and similar morphology of the bubbles in the pebbles regardless of the irradiation temperature. Therefore, to leave the bubbles formed at an irradiation temperature in the range of 686–861 K, tritium atoms have to overcome the same barrier of around 2.7 eV.

Tritium escapes the irradiated beryllium pebble through open channels formed in the microstructure at high temperatures during either irradiation or TPD testing. The lower tritium peak temperatures compared to the helium peaks (see Figs. 4 and 5) are due to the comparatively higher mobility of tritium atoms which faster reach the pebble surface. However, the significant differences in the tritium and helium peak temperatures can mean also that tritium can leave the gas bubbles without formation of open channels. If tritium overcomes the barrier E_A around 2.7 eV, it is able to escape the bubble, to move through the bulk by diffusion, and finally to leave the pebble. In any case, tritium always starts at considerably lower testing temperatures than helium. The presence of a shoulder on the left side of the TPD curves (see Fig. 1a) confirms that here the first-order desorption kinetics occurs because the peak shape has a specific asymmetric shape [21]. An additional release of tritium at lower testing temperatures can be due to

tritium-vacancy (T-V) sub-microscopic clusters or complexes supposedly available in the microstructure along with the gas bubbles. In particular, a shoulder on the left side of the tritium release curve (see Fig. 1a) can be caused by the T-V complexes. Probably, the barrier E_A for these complexes has a lower value compared to the bubble ones therefore tritium is able to leave the complex and then the pebble at comparatively lower temperatures.

Regarding to Fig. 6 it can be revealed that the total tritium release from beryllium pebbles with a diameter of 1 mm decreases by increasing irradiation temperature [15,16]. However, for the pebbles with a diameter of 0.5 mm, the total tritium release is approximately constant despite the increasing temperature and has a significantly lower value to that for 1 mm pebbles. It means that tritium is able effectively to leave the 0.5 mm pebbles at lower irradiation temperatures compared to 1 mm pebbles. The microstructures of 0.5 mm and 1 mm pebbles are very similar, having coarse grains with the close grain size. Therefore, the main factor of the enhanced tritium release from the 0.5 mm pebbles can be relatively less diameter compared to the 1 mm pebbles. This point as well as a difference between values of the tritium desorption energy for 0.5 mm and 1 mm pebbles (2.5 eV and 2.9 eV, accordingly) mean that the use of Redhead method in this study demand more justification. Probably, tritium diffusion and a recapture of tritium after detrapping by other structural traps should be taken into account in future studies. An alternative explana-
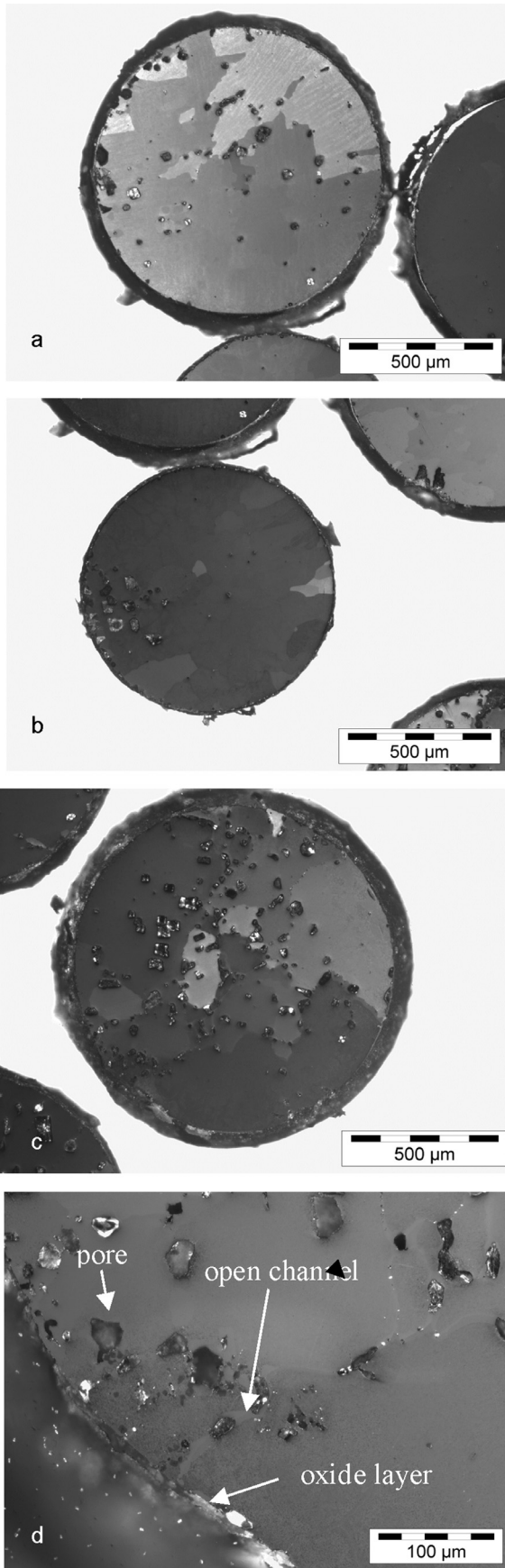
Fig. 15. Optical micrograph in polarized light of cross section of 1 mm beryllium pebble after irradiation at $T_{irr} = 968$ K: (a-c) different modes of pore distribution; (d) open channels and surface oxide layer.
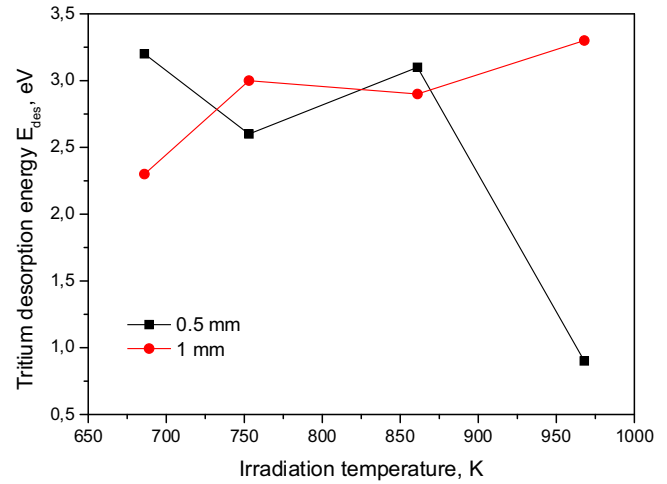

Fig. 16. Tritium desorption energy E_{des} versus irradiation temperature for beryllium pebbles.
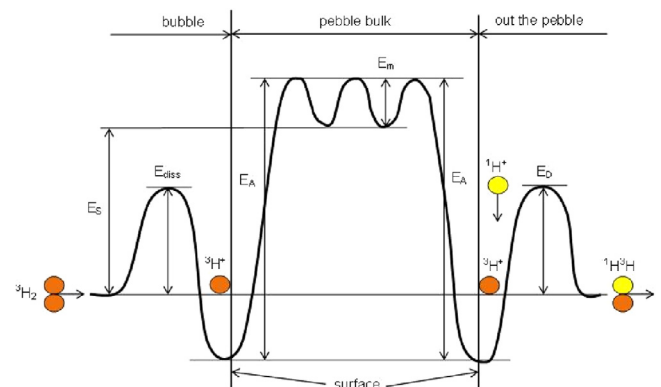

Fig. 17. Potential diagram of tritium in irradiated beryllium.

tion of the difference in the total tritium release values of the 0.5 and 1 mm pebbles can include a possible chemical trapping of tritium due to the beryllium hydroxide formation in the interaction of tritium with beryllium oxide film on the pebble surface [18]. Tritium can escape from the pebble only after dissociation of $Be(OT)_2$. Based on this, the difference above can be explained by the difference of surface areas of these pebbles covered by beryllium oxide layer. However, the beryllium hydroxide presence on the surface of the irradiated beryllium pebbles still has not be found experimentally.

5. Conclusions

After high-dose neutron irradiation of beryllium pebbles with diameters of 0.5 and 1 mm at temperatures of 686–968 K within HIDOBE-01 experiment, the temperature-programmed desorption (TPD) tests with two heating rates of 0.017 K/s and 0.117 K/s were performed. In each tritium and helium release test, only a single release peak was detected. Using peak release temperatures measured at two heating rates, the activation energy of tritium desorption from the irradiated beryllium was calculated by means of Redhead analysis. The tritium desorption energy is 2.7 eV regardless of for the pebble diameter and the irradiation temperature. A clarification of tritium behavior in the irradiated beryllium pebbles based on the calculations of the desorption energy and investigations of the pebble microstructure was suggested. Probably, the transmuted tritium captured during irradiation by structural traps such as small gas bubbles or large pores can escape

the beryllium pebble either through the open channels which are formed in beryllium at high temperatures or by means of detrapping from the structural traps (overcoming the barrier of 2.7 eV) and the following diffusion.

Acknowledgements

References

[1] L.V. Boccaccini, L. Giancarli, G. Janeschitz, S. Hermsmeyer, Y. Poitevin, A. Cardella, E. Diegele, Materials and design of the European DEMO blankets, J. Nucl. Mater. 329–333 (2004) 148–155.
[2] Y. Poitevin, L.V. Boccaccini, M. Zmitko, K. Schleisiek, I. Ricapito, J.-F. Salavy, et al., Tritium breeder blankets design and technologies in Europe: development status of ITER Test Blanket Modules, test & qualification strategy and roadmap towards DEMO, Fusion Eng. Des. 85 (2010) 2340–2347.
[3] V. Chakin, R. Rolli, P. Vladimirov, A. Moeslang, Tritium release from highly neutron irradiated constrained and unconstrained beryllium pebbles, Fusion Eng. Des. 95 (2015) 59–66.
[4] J.B.J. Hegeman, J.G. van der Laan, H. Kawamura, A. Moeslang, I. Kupriyanov, M. Uchida, et al., The HFR Petten high dose irradiation programme of beryllium for blanket application, Fusion Eng. Des 75-79 (2005) 769–773.
[5] S. van Til, J.B.J. Hegeman, H.L. Cobussen, M.P. Stijkel, Evolution of beryllium pebbles (HIDOBE) in long term, high flux irradiation in the high flux reactor, Fusion Eng. Des. 86 (9–11) (2011) 2258–2261.
[6] R.A. Forrest, FISPACT-2003, User Manual. UKAEA FUS 485, December. 2003.
[7] P.A. Redhead, Thermal desorption of gases, Vacuum 12 (1962) 203–211.
[8] J.I. Falconer, R.J. Madix, Flash desorption activation energies: DCOOH decomposition and CO desorption from Ni (110), Surface Sci. 48 (2) (1975) 393–405.
[9] A.M. De Jong, J.W. Niemantsverdriet, Thermal desorption analysis: comparative test of ten commonly applied procedures, Surface Sci. 233 (3) (1990) 355–365.
[10] W.Y. Choo, J Lee, Thermal analysis of trapped hydrogen in pure iron, Metall. Trans. A 13 (1) (1982) 135–140.
[11] M. Klimenkov, V. Chakin, A. Moeslang, R. Rolli, TEM study of beryllium pebbles after neutron irradiation up to 3000 appm helium production, J. Nucl. Mater. 443 (2013) 409–416.
[12] E. Pajuste, A. Vitins, G. Kizane, V. Zubkovs, P. Birjukovs, Tritium distribution and chemical forms in the irradiated beryllium pebbles before and after thermoannealing, Fusion Eng. Des. 86 (2011) 2125–2128.
[13] M.A. Pick, K. Sonnenberg, A model for atomic hydrogen-metal interactions — application to recycling, recombination and permeation, J. Nucl. Mater. 131 (1985) 208–220.
[14] P. Vladimirov, Private communication, September 2015.
[15] A.V. Fedorov, S. van Til, L.J. Magielsen, M.P. Stijkel, Analysis of tritium retention in beryllium pebbles in EXOTIC, PBA and HIDOBE-01 experiments, J. Nucl.Mater 442 (2013) S472–S477.
[16] V. Chakin, R. Rolli, A. Moeslang, M. Klimenkov, M. Kolb, P. Vladimirov, et al., H.-C. Schneider, A.J. Magielsen, Tritium release and retention properties of highly neutron-irradiated beryllium pebbles from HIDOBE-01 experiment,, J. Nucl. Mater 442 (2013) 483–489.
[17] E. Rabaglino, J.P. Hiernaut, C. Ronchi, F. Scaffidi-Argentin, Helium and tritium kinetics in irradiated beryllium pebbles, J. Nucl. Mater 307–311 (2002) 1424–1429.
[18] F. Scaffidi-Argentina, Tritium and helium release from neutron irradiated beryllium pebbles from the EXOTIC-8 irradiation, Fusion Eng. Des 58-59 (2001) 641–645.
[19] E. Rabaglino, J. Baruchel, E. Boller, A. Elmoutaouakkil, C. Ferrero, C. Ronchi, et al., Study by microtomography of 3D porosity networks in irradiated beryllium, Nucl. Instrum. Methods Phys. Res. B 200 (2003) 352–357.
[20] F. Scaffidi-Argentina, G. Piazza, R. Rolli, Microstructural analysis of beryllium samples irradiated at high temperature, Fusion Eng. Des. 69 (2003) 505–509.
[21] C.-M. Chan, R. Aris, W.H. Weinberg, An analysis of thermal desorption mass spectra. I, Appl. Surface Sci. 1 (1978) 360–376.